Bright-to-dark-to-bright photoisomerisation in a forked (phenylene ethynylene) dendrimer prototype and its building blocks: a new mechanistic shortcut for excitation-energy transfer?

G. Breuil, Thibaud Etienne, Benjamin Lasorne

Bright-to-dark-to-bright photoisomerisation in a forked (phenylene ethynylene) dendrimer prototype and its building blocks: A new mechanistic shortcut for excitation-energy transfer?

G. Breuil,[1] T. Etienne*,[2] and B. Lasorne*[1]
[1)]*ICGM, Univ Montpellier, CNRS, ENSCM, Montpellier, France*
[2)]*LPCT, Univ Lorraine, CNRS, Vandoeuvre-lès-Nancy, France*

(*Electronic mail: benjamin.lasorne@umontpellier.fr)

(*Electronic mail: thibaud.etienne@univ-lorraine.fr)

(Dated: January 26, 2023)

Dendrimers made of oligo(phenylene ethynylene) building blocks are highly-organised two-dimensional macromolecules that have raised much interest for their potential use as artificial light-harvesting antennae. Excitation-energy transfer is assumed to occur from the periphery to the core via a tree-shaped graph connecting a pair of donors on each acceptor. The received photophysical mechanism involves a converging cascade of crossings among bright electronic states foremost mediated by rigid acetylenic stretching modes. On the other hand, competition with in-plane *trans*-bending motions has been detected experimentally in oligomers and confirmed by computations in larger species, thus suggesting the additional involvement of dark electronic states acting as intermediates. In the present work, we show that this secondary process represents an alternative pathway that may not be detrimental and could even be viewed as a mechanistic shortcut.

I. INTRODUCTION

Poly(phenylene ethynylene) (PPE) – or more generally poly(arylene ethynylene) (PAE) – polymers are well-established commercial materials known for their outstanding properties as light-emitting polymers, especially in the context of technologies based on π-conjugated organic optoelectronics involving OLEDs (small-molecule organic light-emitting diodes) and PLEDs (polymer OLEDs).[1]

Closely related, dendrimers[2,3] of phenylene ethynylene (DPEs) have attracted much attention over the last decades as potential candidates for acting as artificial light-harvesting macromolecules, the most famous one to date being the so-called "nanostar", which exhibits enhanced fluorescence from its perylene core by design.[4–10]

Typically, natural and biomimicking light-harvesting systems are supramolecular assemblies that absorb light in the UV-visible domain at the one end, further channel excitation-energy transfer (EET) through a sequence of through-space weakly-coupled donors and acceptors, and release the absorbed energy at the other end for conversion into useful work (see, for example, Ref. 11).

DPEs show similar light-harvesting properties, but they present two specific features: first, they are single covalent macromolecules; second, their branched connectivity should make them capable of through-bond EET amplification or concentration. Indeed, they are organised according to tree-shaped connected graphs made of similar subunits of increasing length from the periphery to the core. Each subunit consists in a π-conjugated linear oligo(phenylene ethynylene) (oPE) chromophore, typically with two, three, and four rings. They are linked together through threefold *meta*-substitution on shared phenylene nodes such that each node gathers two identical energy donors (D) and one energy acceptor (A), yielding a macromolecular architecture based on nested layers of DDA-type connections (see Ref. 12).

EET in DPEs is thus governed by a convergent flow of unidirectional excitation-energy gradients due to the decrease of the energy gap when the size of the conjugated π-system of a linear oPE chromophore increases and is expected to travel, gather, and concentrate via each node through the tree, basically from the "leaves" to the "trunk".

It must be stressed that the decomposition of DPEs into an assembly of weakly-interacting oPE donors and acceptors has become well accepted over the years but is not so evident from the onset. Adjacent donors and acceptors meeting at nodes within the tree-like architecture cannot be fragmented into actual oPE moieties, since they all share common phenylene rings; in addition, they are expected to exhibit strong π-conjugation extended over the whole system at first sight.

However, experimental studies have definitively shown that the absorption spectrum in the UV domain of the prototypical "nanostar" for example was almost identical to the superposition of the first absorption bands of its linear oPE branches (two, three, and four rings) plus that of the perylene core.[4–6,8,10] It thus occurs that DPEs actually behave as if they were made of a branched array of aggregated oPEs interacting weakly together.

This apparent paradox can in fact be rationalised easily using what we termed a pseudo-fragmentation scheme in a recent study.[13] The latter work exemplified this concept on 1,3-bis(phenylethynyl)benzene where the two overlapping oPE pseudo-fragments are tolane (aka. diphenylacetylene: DPA) molecules. The rationale for pseudo-fragmentation is the participation to the π-conjugation of two distinct pairs of degenerate frontier orbitals on each *meta*-substituted phenylene ring (one re-hybridised for the left, the other for the right) instead of a single pair on a *para*-substituted one (equally shared and delocalised equally to the left and to the right). For this reason, each *meta*-phenylene node can be viewed eventually as a "double site".

Quite obviously, understanding the detailed electronic

properties and photodynamics of basic oPE subunits within DPEs is of fundamental importance in order to find optimal conditions for EET to occur and be amplified efficiently in such macromolecules. For this, we address in the present work an aspect that has not been prominently investigated in the literature on DPEs: namely, the potential photoisomerisation from bright to dark (and from dark to bright) states via in-plane bending motions of acetylenic moieties, within the rigid network of benzene rings, leading to the intermediate formation of *trans*-stilbene-like biradicals in forked species.

Indeed, it has been shown with time-resolved spectroscopy by Hirata et al., already in the 1990's,[14] and further confirmed by later experimental and theoretical studies[15–18] that tolane could experience — after a transition to its first-excited bright singlet electronic state — some nonnegligible photoconversion into a more stable dark *trans*-stilbene-like photoisomer on a few-picosecond time scale. Later on, Fujiwara et al.[19] have shown that the next member in the series, the three-ring *para*-linear oPE, 1,4-bis(phenylethynyl)benzene, could in principle experience a similar photoisomerisation but much less efficiently, due to a much higher activation energy and a reverted stabilisation energy order between both bright and dark isomers.

The present work is a computational and theoretical study where we show how the results and interpretation of previous studies on the first two linear oPEs will help in understanding how photoisomerisation among bright and dark states may affect EET in the first dendrimer-like "forked DDA-type" prototype, namely 1,3,5-bis(phenylethynyl)(diphenylethynyl)benzene (a pair of two donors on a single threefold-ring acceptor).

We expect the results presented in the present study to be viewed as first and crucial insights into further addressing possible competition between EET and photoisomerisation within extended DPEs in a more detailed way than the ideal scheme, which we also investigated recently in Ref. 20, based on a cascade of bright states mediated by rigid stretching modes.

II. COMPUTATIONAL DETAILS

We performed DFT and linear-response TD-DFT calculations within the CAM-B3LYP/6-31+G(d) level of theory, previously assessed for tolane,[21] extended to other members of the series including 1,4-bis(phenylethynyl)benzene,[22] and further applied to 1,3-bis(phenylethynyl)benzene,[13] using the Gaussian quantum chemistry package, version 16, Revision A.03.[23]

Vibrationnally resolved absorption spectra (so-called "vibronic" spectra) were calculated via the standard Franck-Condon-Herzberg-Teller (FCHT) module of Gaussian[24] for the three linear species within the harmonic, Born-Oppenheimer, and Franck-Condon approximations. We showed in Ref. 22 (following early prescriptions laid out in Ref. 21) that the 0–0 band origins and the dominant vibrational progressions were in very good agreement with experimental data, using the aforementioned level of theory, for tolane and those of each *para*-oligo(phenylene ethynylene), in particular 1,4-bis(phenylethynyl)benzene of interest here.

Minimum and transition-state geometries were optimised in ground and excited electronic states and characterised with frequency calculations for the three systems.

Minimum-energy conical intersections (MECIs) between bright and dark states were optimised with the method presented in Ref. 25. It was originally proposed for singlet/triplet crossings for which the spin-orbit-coupling-free branching space is one-dimensional. We applied it within geometrical subspaces where both singlet states have different spatial symmetries, such that the derivative coupling describes a non-totally-symmetric direction and, as such, is orthogonal to the energy gradients by construction.

Finally, we calculated derivative couplings numerically with the procedure exposed in Ref. 26, based on a harmonic analysis of the Hessian of the squared energy difference.

The "nature" of the relevant electronic states at representative molecular geometries was further characterised with electron-density-based descriptors, calculated according to the formalism and methodology exposed in Refs. 27–29 and implemented in the MESRA code.[30]

Such descriptors are essentially based on the analysis of the unrelaxed one-body reduced difference density matrix obtained as the difference between the one-body reduced density matrices of the two electronic states of interest.[31] The depleted and accumulated density contributions, with possible overlap, are termed "detachment" and "attachment" densities.[29,32]

Our first descriptor is the amount of charge transferred during the electronic transition (the integral of the positive – or equivalently, the absolute value of the negative – contributions to the difference density). It is typically known as q^{CT}.[28,31] Our second descriptor, ϕ_S, measures the locality of the density rearrangement: it is defined as the spatial overlap between the detachment and the attachment densities.[27]

III. RESULTS AND DISCUSSION

The pseudofragmentation scheme developed by Ho and Lasorne[13] allows us to describe a DPE as if its oPE branches were excitation-energy donors (D) and acceptors (A) (pseudofragments), weakly interacting together, when bright electronic states are concerned. We shall see below that this also applies to dark electronic states.

A. Linear oPEs

Let us start with the three smallest oPEs: DPA (diphenylacetylene, aka. tolane), BPEB (1,3-bis(phenylethynyl)benzene), and DPABPEB (next linear species with four rings). Their ground-state Lewis structures at equilibrium geometries are given in Fig. 1.

They are all highly π-conjugated species, with aromatic phenylene groups being spaced by alternated single-triple-single bonds. They all belong to the $\mathscr{D}_{2h}$ point group. The

Mulliken convention will be used thereafter, such that the z-axis is the C_2-axis, and the x-axis is orthogonal to the molecular plane. The ground electronic state of each system is then 1^1A_g (closed shell).

The first adiabatic electronic excited singlet states of DPA have been studied both experimentally and theoretically.[14–18,22,33–36] At the ground-state equilibrium geometry (also called the Franck-Condon − FC − geometry), the first optically active (bright) state is 1^1B_{1u}. It lies around $4-5$ eV, where five electronic excited states have been characterised (1^1B_{1u}, 1^1B_{2u}, 1^1B_{3g}, 1^1A_u, and 2^1A_g). There is no definitive consensus on their exact energy ordering, but only 1^1B_{1u} is bright; it corresponds to a typical $\pi-\pi^*$ locally excited (LE) transition with a strong oscillator strength, as expected. We shall call the first singlet adiabatic excited state S_1.

The minimum geometry of 1^1B_{1u} corresponds to a cumulenic bonding pattern (a sequence of three double bonds along orthogonal planes) surrounded by quinoidal rings (see Fig. 1). It will be further named as the cumulenic isomer, *c*DPA.

It is now received knowledge that *c*DPA is the precursor of another optically inactive (dark) species in S_1, *t*DPA, associated to a *trans*-isomer (see Fig. 1), according to the experimental evidence provided by Hirata *et al.*,[14] where they proposed a photoisomerisation mechanism: $S_0 \rightarrow X \rightarrow Y \rightarrow T_1$ in which S_0 is ground-state DPA, X is S_1 *c*DPA (bright), Y is S_1 *t*DPA (dark), and T_1 is a subsequent triplet species. This was further confirmed by theoretical studies.[15–17,35]

The dark isomer belongs to the $\mathscr{C}_{2h}$ point group where S_1 is 1^1A_u. Its energy is lower than that of the bright $\mathscr{D}_{2h}$ isomer where S_1 is 1^1B_{1u} (1^1B_u in $\mathscr{C}_{2h}$, while 1^1A_u in $\mathscr{C}_{2h}$ correlates with a mixture of 1^1B_{3u} and 2^1A_u in $\mathscr{D}_{2h}$).

Our TD-CAM-B3LYP/6-31+G(d) calculations show that $S_1/1^1B_{1u}$ at the FC point lies at 4.476 eV (oscillator strength $f = 0.93$) above the ground-state minimum, while the corresponding *c*DPA S_1 isomer (local minimum) is at 4.144 eV (oscillator strength $f = 0.96$); the dark *t*DPA S_1 isomer (global minimum) is at 3.716 eV (see Table I).

Less information is to be found in the literature on the cumulenic and *trans* isomers of BPEB. As opposed to DPA, the minimum of the dark state (1^1A") is now higher in energy than the bright state (1^1B_{1u}). In particular, Fujiwara *et al.*[19] have found that the bright *c*PBEB S_1 isomer is at 3.25 eV and the dark *t*PBEB S_1 isomer is at 3.51 eV, while Hodecker *et al.*[37] have obtained 3.90 eV and 4.25 eV, respectively.

Our level of theory places them in between, at 3.624 eV (oscillator strength $f = 2.00$) and 3.685 eV (oscillator strength $f = 0.00$); see table I. The three levels of theory (BP86/cc-pVDZ,[19] CAM-B3LYP/def2-TZVP,[37], and CAM-B3LYP/6-31+G(d) in the present work) give consistent trends in terms of energy ordering.

No similar data have been found in the literature for the longer linear species with four rings, DPABPEB. Our present calculations identified consistently a $\mathscr{D}_{2h}$ S_0 equilibrium geometry (bright FC $S_1/1^1B_{1u}$ at 3.626 eV). The bright $\mathscr{D}_{2h}$ isomer (*c*-DPABPEB; see Fig. 1) 1^1B_{1u} lies at 3.376 eV. There are now two distinct dark *trans* isomers in S_1: the peripheral-*trans* isomer (*peri t*-DPABPEB) and the middle-*trans* isomer (*mid t*-DPABPEB); see Fig. 1. The first one is $\mathscr{C}_s$ and corresponds to a dark 1^1A" state (3.687 eV). The second one is $\mathscr{C}_{2h}$ and corresponds to a 1^1A_u dark state, slightly lower in energy (3.652 eV).

The three oPE linear systems (with two, three, and four rings) in S_1 at the FC geometry (vertical transitions) and at their cumulenic geometries (bright isomers) are all characterised by a large oscillator strength (see Table II). The corresponding excited electronic states are all of $\pi-\pi^*$ LE character, described by a dominant HOMO/LUMO transition; see Fig. 2. The reorganisation of all bonding patterns from alternated-aromatic to cumulenic-quinoidal is consistent with the excited Lewis structures given in Fig. 1 and with changes in equilibrium geometries from S_0 to the bright S_1.

In a more quantitative manner, this can be characterised upon examining the attachment and detachment densities[27–32] shown in Fig. 3. First, they are upon visual inspection almost identical to the squares of the HOMO and LUMO for each system. This means that the electronic transition can be pictured approximately as if a single electron of the HOMO were excited to the LUMO (excitonic approximation). The attachment-detachment-overlap density-based descriptor, ϕ_S,[27] is equal to 0.86 in the case of DPA, 0.85 for both BPEB and DPABPEB, consistent with LE states of similar character.

In addition, the other relevant charge-shift density-based descriptor, q^{CT},[28,31] gives similar values for the three systems: approximately 0.4 (see Fig. 3), which means than the net spatial charge displacement involved in the photoexcitation is low, again consistent with a strong LE character: the density is locally reorganised through space but does not involve the creation of any significant electric dipole over the extent of the molecule.

Let us now consider the dark isomers in S_1. Their equilibrium geometries are characterised by a HOMO/LUMO pair (see Fig. 4) that differ much from the cumulenic isomers: the LUMOs of the cumulenic and *trans* isomers involve the orthogonal π_x^* molecular orbital and the parallel π_y^* molecular orbitals, respectively. The LUMOs of the *trans* isomers are thus in-plane and very much localised on a singly-bent ethynylene group. As a consequence, the *trans* isomers of all species almost have the same energy, irrespective of the number of rings: ~ 3.7 eV (see table I).

The attachment and detachment densities shown in Fig. 5 have quite similar shapes to the HOMO/LUMO pairs associated to each oPE, except that they are more localised on the ethynylene groups that are actually bent. The attachment-detachment-overlap descriptors take values that are lower than those of the cumulenic isomers ($\phi_S = 0.53-0.54$ in all cases), while the charge-shift descriptors take values that are greater ($q^{CT} = 0.74-0.75$ in all cases). Dark isomers can be viewed as if almost one electron were displaced upon transition from the orthogonal π-plane to the parallel σ-plane, thus yielding a biradicaloid species that is the direct precursor of a triplet (much similar to dioxygen).

Let us now consider continuous geometric displacements connecting the various bright and dark isomers in S_1. Four "rigid scans" are gathered in Fig. 6 along the γ-angle, defined such that it is the symmetrical bending angle centred on

	FC point	cumulenic isomer	*trans* isomer
DPA	1^1B_{1u} : 4.476	1^1B_{1u} : 4.144	1^1A_u : 3.716
BPEB	1^1B_{1u} : 3.896	1^1B_{1u} : 3.624	1^1A" : 3.685
DPABPEB	1^1B_{1u} : 3.626	1^1B_{1u} : 3.376	1^1A" : 3.687 (*peri t*)
			1^1A_u : 3.652 (*mid t*)

Table I. Energies (in eV) and state symmetries of the Franck-Condon points and of the cumulenic and *trans* isomers, relative to the ground-state minimum, for DPA, BPEB, and DPABPEB.

	cumulenic isomer	*trans* isomer
DPA	0.96	0.00
BPEB	2.00	0.00
DPABPEB	2.94	0.00 (*peri t*)
		0.00 (*mid t*)

Table II. Oscillator strength (f) of the cumulenic and *trans* isomers (minima in their first adiabatic electronic excited states).

a cumulenic CCCC group. They are originated from the S_1 cumulenic (bright) isomers.

We observe three apparent minima in S_1 for each case. At $\gamma = 180°$, the actual equilibrium geometry is the optimised cumulenic ($\mathscr{D}_{2h}$ linear) one. On the left and on the right, there are two other apparent *trans*-minima located around $\gamma \sim 130°$ and $\gamma \sim 230°$ (the corresponding re-optimised *trans*-isomers are in fact all defined by an angle of $\gamma = 128°$ and $\gamma = 232°$). We hence observe expected S_2/S_1 conical intersections between bright and dark states around $\gamma \sim 140-150°$ and $\gamma \sim 210-220°$ (see Table III).

	Rigid scan	Optimised
t-DPA	4.523 - 150°	4.443 - 152°
t-BPEB	4.393 - 142°	4.189 - 148°
peri t-DPABPEB	4.439 - 137°	-
mid t-DPABPEB	4.258 - 140°	-

Table III. Relative energies (eV) and γ values of the apparent (along rigid scans) and optimised (minimum energy) bright/dark conical intersections between S_1 and S_2.

Note that "rigid" conical intersections are good approximations to the optimised ones. However, we know that increasing the size of an oPE tends to lower the energy of the bright state, leading to smaller γ values for the crossing with the dark state, the energy of which is not affected by the size of the system, as illustrated in Fig. 7.

B. Singly *meta*-substituted oPE

Let us now focus on the smallest *meta*-substituted species that we shall further call *m*-BPEB (its pseudofragments are two DPAs). There is no net excitation energy transfer (EET), but *m*-BPEB is the prototype for pseudofragmentation.

The first two bright states of *m*-BPEB in the $\mathscr{C}_{2v}$ point group (1^1B_2 and 2^1A_1) are both LE states.[13] At the ground-state equilibrium geometry (FC point), 1^1B_2 lies at 4.43 eV ($f = 1.71$) and 2^1A_1 at 4.47 eV ($f = 0.37$). The lowest $\mathscr{C}_{2v}$ energy-points in S_1 are two transition states, TS_{A_1} and TS_{B_2}. They occur at 4.29 eV and 4.25 eV, respectively. Both states cross at a $\mathscr{C}_{2v}$ minimum-energy CoIn point, at 4.29 eV, near TS_{A_1}.

We calculated the two density-based descriptors at TS_{A_1} and TS_{B_2}: $\phi_S(TS_{B_2}) = 0.86$, $q^{CT}(TS_{B_2}) = 0.36$, and, $\phi_S(TS_{A_1}) = 0.87$, $q^{CT}(TS_{A_1}) = 0.35$, consistent with a strong and similar LE character for both states (large attachment-detachment overlap and small net charge shift).

The minimum-energy CoIn point between the 1^1B_2 and 2^1A_1 states in $\mathscr{C}_{2v}$ brings a pair of branching-space vectors (both directions along which degeneracy is lifted to first order) defined such that the gradient half-difference, $\overrightarrow{GD}$ vector, preserves the $\mathscr{C}_{2v}$ point group (A_1), and the derivative coupling, $\overrightarrow{DC}$ vector, lowers the symmetry so as to mix both states maximally (B_2) and turns them into $1^1A'$ and $2^1A'$ at the pair of equivalent $\mathscr{C}_s$ S_1 minima.

Consistently, the S_1 state is characterised by two equivalent bright isomers with $\mathscr{C}_s$ broken symmetry on either side: one of the two ethynylene groups has cumulenic bonds and quinoidal phenylene groups while the other side remains unchanged (denoted *c*-*m*-BPEB in Fig. 8, while distinguishable dark *trans*-isomers are denoted *it*-*m*-BPEB for "inside" and *ot*-*m*-BPEB for "outside").

The attachment and detachment densities computed at TS_{B_2} and TS_{A_1} are very similar. However, at *c*-*m*BPEB, they become much localised on the excited branch (see Fig. 9). Structural similarities between *c*-*m*-BPEB and *c*-DPA in S_1 are reflected in the values of the two density-based descriptors for the bright species: $\phi_S = 0.86$ and $q^{CT} = 0.36$. In contrast, $\phi_S = 0.54$ and $q^{CT} = 0.73$ for the dark species: *t*DPA, $it-m$BPEB, and $ot-m$BPEB.

C. Forked and doubly (*meta bis*)-substituted oPE

The first DDA-type forked DPE species – now able to exhibit EET from DD to A, which we investigated in Ref. 20 – will be further denoted *mb*-DPABPEB. Its equilibrium geometries in S_0 and S_1 (bright) both belong to the $\mathscr{C}_{2v}$ point group, and to $\mathscr{C}_s$ in S_2 (bright); corresponding Lewis structures are shown in Fig. 10.

The first bright minimum in S_1 is localised on the "long branch": it is a $\mathscr{C}_{2v}$ structure (see middle panel in Fig. 10) that corresponds to the 2^1A_1 state at 3.591 eV (similar to the

BPEB 1^1B_{1u} cumulenic minimum at 3.624 eV; see table IV). The second bright minimum of *mb*-DPABPEB in S_2 (see right panel in Fig. 10) corresponds to an excitation on one or the other two equivalent short branches, hence a pair of mirror-image minima of $\mathscr{C}_s$ symmetry at 4.142 eV (similar to *m*-BPEB ($2^1A'$, 4.123 eV) and DPA (1^1B_{1u}, 4.144 eV); see table IV).

The bright S_2 state at its equilibrium geometry (see right panel in Fig. 10) is characterised by several single excitations among the near-frontier orbitals (HOMO−1, HOMO, LUMO, and LUMO+1), as shown in Fig. 11: in particular, HOMO $\rightarrow$ LUMO (44%), HOMO $-1 \rightarrow$ LUMO $+1$ (19%), and HOMO $-1 \rightarrow$ LUMO (16%). The corresponding natural transition orbitals (NTOs) provide a more compact representation by definition (see Fig. 11) and show a dominant excitation pair with a singular value of 85%, consistent with the localisation of the detachment and attachment densities on the same DPA pseudofragment branch.

Let us now examine how the *mb*-DPABPEB molecule behaves regarding *trans*-bending, either along its short or long branches, and how dark bent isomers connect with various cumulenic bright isomers.

The "rigid scans" shown in Fig. 12 were performed from the bright minimum (short-branch cumulenic equilibrium geometry in S_2) for various systems having a short pseudofragment (two rings).

In contrast, the "rigid scans" shown in Fig. 13 were performed from the bright minimum (long-branch cumulenic equilibrium geometry in S_1) for various systems having a long pseudofragment (three rings).

The rigid scans (a) to (d) in Fig. 12 have been performed along the bending angle γ for all systems having an excited linear two-ring oPE (DPA) pseudofragment: namely, DPA (a), *m*-BPEB (b), *m*-DPABPEB (c), and *mb*-DPABPEB (d). The starting geometries were those of bright cumulenic species, typically in S_2 (donor). In contrast, the rigid scans (a) to (e) in Fig. 13 have been performed along γ for all systems having an excited linear three-ring oPE (BPEB) pseudofragment: namely, BPEB (a), *m*-DPABPEB inside (b) and outside (c), *mb*-DPABPEB inside (d) and outside (e). The starting geometries were those of bright cumulenic species, typically in S_1 (acceptor).

In order to evaluate EET efficiency between the bright and dark states, we evaluated the magnitude of the derivative coupling (DC) vectors at relevant crossings points and compared them to the magnitudes of the corresponding gradient (half) difference (GD) vectors.

For all systems of interest, a crossing between the cumulenic (bright) and *trans* (dark) isomers along the same branch corresponds to $|| \overrightarrow{DC} || = 0.03 - 0.04\ E_h a_0^{-1}$ and $|| \overrightarrow{GD} || = 0.08 - 0.09\ E_h a_0^{-1}$, hence a ratio approximately equal to one half (bright-to-dark: potentially quite efficient)

In contrast, a crossing between the cumulenic (bright) and *trans* (dark) isomers along two adjacent branches corresponds to $|| \overrightarrow{DC} || = 0.01 - 0.02\ E_h a_0^{-1}$ and $|| \overrightarrow{GD} || = 0.13\ E_h a_0^{-1}$, hence a ratio approximately equal to one tenth (dark-to-bright: not major but sufficiently efficient to be considered).

On the other hand, two cumulenic bright states $1^1B_2/2^1A_1$ in the same species are strongly coupled with each other: $|| \overrightarrow{DC} || = 0.14\ E_h a_0^{-1}$ and $|| \overrightarrow{GD} || = 0.03\ E_h a_0^{-1}$, where the ratio is equal to five (direct bright-to-bright: potentially very efficient).

We thus propose a – perhaps more complicated than the received one, based on bright states only – but richer de-activation mechanism involving a cascade of bright-to-dark-to bright crossings, as summarised in Fig. 14.

It must be stressed that connecting one or two short oPEs onto a long one (as in the asymmetrical DA-type *m*-DPABPEB and the symmetrical and forked DDA-type *mb*-DPABPEB species; see Figs. 13 and 12) eventually provides an ultrafast "escape" route from the *trans* dark intermediate species, which otherwise could act as a "dead end" or – perhaps worst – an early precursor for triplet formation, much as in the unsubstituted DPA.

Indeed, all cases show that the cumulenic bright state on the "long" species (three rings) BPEP makes it the final acceptor state for EET (always lower in energy when geometrically relaxed; see Fig. 13). The now remaining and unsolved question concerns the detailed kinetic sequence induced among the higher-energy donor states up to this energy trap.

IV. CONCLUSIONS AND OUTLOOK

Our study makes us suggest that EET in DPEs not only is driven by rigid skeletal deformations of the carbon backbone but also may be affected by *trans*-bending motions, which could provide a shortcut between bright states via dark states on different sites.

This has been assessed from various perspectives, including topological density-based descriptors, as well as a comparison between the relative norms of branching-space vectors at various crossing points.

As expected from such systems, the properties of various small pseudofragments are to be observed in larger species, as if linear donor and acceptor chromophores were weakly coupled.

We thus are now in a position to propose a perhaps more complicated – yet richer – de-activation mechanism involving a secondary cascade of bright-to-dark-to-bright crossings and photoisomerisations competing with the primary, direct, bright-to-bright cascade of internal conversions along excited oPE sequences. Such a scenario based on a mechanistic shortcut that yields lower activation energies, while involving the potential benefit of inducing local disorder through the ideally organised network, now awaits further confirmation from both time-resolved transient spectroscopy and quantum-dynamics simulations.

ACKNOWLEDGMENTS

The authors wish to acknowledge scientific and financial support from the GDR UP network and the French Ministry of Higher Education and Research for funding the PhD thesis of GB.

	mb-DPABPEB	*m*-BPEB	BPEB	DPA
short cumulenic	$2^1A'$: 4.142	$2^1A'$: 4.123	-	1^1B_{1u}: 4.144
short *trans*	1^1A": 3.737	1^1A": 3.726	-	1^1A_u: 3.716
	1^1A": 3.736	1^1A": 3.728		
long cumulenic	2^1A_1: 3.591	-	1^1B_{1u}: 3.624	-
long *trans*	1^1A" : 3.699	-	1^1A" : 3.685	-
	1^1A" : 3.694			

Table IV. Relative energies (in eV) and state symmetries of relevant and related isomers of *mb*-DPABPEB, *m*-BPEB, BPEB, and DPA.

DATA AVAILABILITY

The datasets generated during and/or analysed during the current study are available from the corresponding author on reasonable request.

REFERENCES

[1] C. Weder and G. Voskerician, "Electronic Properties of PAEs," in *Poly(arylene etynylene)s: From Synthesis to Application*, Advances in Polymer Science, edited by C. Weder (Springer, Berlin, Heidelberg, 2005) pp. 209–248.

[2] A. Bar-Haim, J. Klafter, and R. Kopelman, "Dendrimers as Controlled Artificial Energy Antennae," J. Am. Chem. Soc. **119**, 6197–6198 (1997), publisher: American Chemical Society.

[3] D. Astruc, E. Boisselier, and C. Ornelas, "Dendrimers Designed for Functions: From Physical, Photophysical, and Supramolecular Properties to Applications in Sensing, Catalysis, Molecular Electronics, Photonics, and Nanomedicine," Chem. Rev. **110**, 1857–1959 (2010), publisher: American Chemical Society.

[4] R. Kopelman, M. Shortreed, Z.-Y. Shi, W. Tan, Z. Xu, J. S. Moore, A. Bar-Haim, and J. Klafter, "Spectroscopic Evidence for Excitonic Localization in Fractal Antenna Supermolecules," Phys. Rev. Lett. **78**, 1239–1242 (1997), publisher: American Physical Society.

[5] M. R. Shortreed, S. F. Swallen, Z.-Y. Shi, W. Tan, Z. Xu, C. Devadoss, J. S. Moore, and R. Kopelman, "Directed Energy Transfer Funnels in Dendrimeric Antenna Supermolecules," J. Phys. Chem. B **101**, 6318–6322 (1997), publisher: American Chemical Society.

[6] V. D. Kleiman, J. S. Melinger, and D. McMorrow, "Ultrafast Dynamics of Electronic Excitations in a Light-Harvesting Phenylacetylene Dendrimer," J. Phys. Chem. B **105**, 5595–5598 (2001), publisher: American Chemical Society.

[7] E. Atas, Z. Peng, and V. D. Kleiman, "Energy Transfer in Unsymmetrical Phenylene Ethynylene Dendrimers," J. Phys. Chem. B **109**, 13553–13560 (2005), publisher: American Chemical Society.

[8] J. L. Palma, E. Atas, L. Hardison, T. B. Marder, J. C. Collings, A. Beeby, J. S. Melinger, J. L. Krause, V. D. Kleiman, and A. E. Roitberg, "Electronic Spectra of the Nanostar Dendrimer: Theory and Experiment," J. Phys. Chem. C **114**, 20702–20712 (2010), publisher: American Chemical Society.

[9] J. Huang, L. Du, D. Hu, and Z. Lan, "Theoretical analysis of excited states and energy transfer mechanism in conjugated dendrimers," Journal of Computational Chemistry **36**, 151–163 (2015), _eprint: https://onlinelibrary.wiley.com/doi/pdf/10.1002/jcc.23778.

[10] V. M. Freixas, D. Ondarse-Alvarez, S. Tretiak, D. V. Makhov, D. V. Shalashilin, and S. Fernandez-Alberti, "Photoinduced non-adiabatic energy transfer pathways in dendrimer building blocks," J. Chem. Phys. **150**, 124301 (2019), publisher: American Institute of Physics.

[11] C. Azarias, L. Cupellini, A. Belhboub, B. Mennucci, and D. Jacquemin, "Modelling excitation energy transfer in covalently linked molecular dyads containing a BODIPY unit and a macrocycle," Phys. Chem. Chem. Phys. **20**, 1993–2008 (2018), publisher: The Royal Society of Chemistry.

[12] S. Tomasi and I. Kassal, "Classification of Coherent Enhancements of Light-Harvesting Processes," J. Phys. Chem. Lett. **11**, 2348–2355 (2020), publisher: American Chemical Society.

[13] E. K. L. Ho and B. Lasorne, "Diabatic pseudofragmentation and nonadiabatic excitation-energy transfer in meta-substituted dendrimer building blocks," Computational and Theoretical Chemistry **1156**, 25–36 (2019).

[14] Y. Hirata, T. Okada, N. Mataga, and T. Nomoto, "Picosecond time-resolved absorption spectrum measurements of the higher excited singlet state of diphenylacetylene in the solution phase," J. Phys. Chem. **96**, 6559–6563 (1992), publisher: American Chemical Society.

[15] M. Z. Zgierski and E. C. Lim, "Nature of the 'dark' state in diphenylacetylene and related molecules: state switch from the linear state to the bent state," Chemical Physics Letters **387**, 352–355 (2004).

[16] J. Saltiel and V. K. R. Kumar, "Photophysics of Diphenylacetylene: Light from the "Dark State"," J. Phys. Chem. A **116**, 10548–10558 (2012), publisher: American Chemical Society.

[17] M. Krämer, U. H. F. Bunz, and A. Dreuw, "Comprehensive Look at the Photochemistry of Tolane," J. Phys. Chem. A **121**, 946–953 (2017), publisher: American Chemical Society.

[18] C. Robertson and G. A. Worth, "Modelling the non-radiative singlet excited state isomerization of diphenyl-acetylene: A vibronic coupling model," Chemical Physics **510**, 17–29 (2018).

[19] T. Fujiwara, M. Z. Zgierski, and E. C. Lim, "Spectroscopy and Photophysics of 1,4-Bis(phenylethynyl)benzene: Effects of Ring Torsion and Dark * State," J. Phys. Chem. A **112**, 4736–4741 (2008), publisher: American Chemical Society.

[20] G. Breuil, E. Mangaud, B. Lasorne, O. Atabek, and M. Desouter-Lecomte, "Funneling dynamics in a phenylacetylene trimer: Coherent excitation of donor excitonic states and their superposition," J. Chem. Phys. **155**, 034303 (2021), publisher: American Institute of Physics.

[21] C. Adamo and D. Jacquemin, "The calculations of excited-state properties with Time-Dependent Density Functional Theory," Chem. Soc. Rev. **42**, 845–856 (2013), publisher: The Royal Society of Chemistry.

[22] E. K.-L. Ho, T. Etienne, and B. Lasorne, "Vibronic properties of para-polyphenylene ethynylenes: TD-DFT insights," J. Chem. Phys. **146**, 164303 (2017), publisher: American Institute of Physics.

[23] M. J. Frisch, G. W. Trucks, H. B. Schlegel, G. E. Scuseria, M. A. Robb, J. R. Cheeseman, G. Scalmani, V. Barone, G. A. Petersson, H. Nakatsuji, X. Li, M. Caricato, A. V. Marenich, J. Bloino, B. G. Janesko, R. Gomperts, B. Mennucci, H. P. Hratchian, J. V. Ortiz, A. F. Izmaylov, J. L. Sonnenberg, D. Williams-Young, F. Ding, F. Lipparini, F. Egidi, J. Goings, B. Peng, A. Petrone, T. Henderson, D. Ranasinghe, V. G. Zakrzewski, J. Gao, N. Rega, G. Zheng, W. Liang, M. Hada, M. Ehara, K. Toyota, R. Fukuda, J. Hasegawa, M. Ishida, T. Nakajima, Y. Honda, O. Kitao, H. Nakai, T. Vreven, K. Throssell, J. A. Montgomery, Jr., J. E. Peralta, F. Ogliaro, M. J. Bearpark, J. J. Heyd, E. N. Brothers, K. N. Kudin, V. N. Staroverov, T. A. Keith, R. Kobayashi, J. Normand, K. Raghavachari, A. P. Rendell, J. C. Burant, S. S. Iyengar, J. Tomasi, M. Cossi, J. M. Millam, M. Klene, C. Adamo, R. Cammi, J. W. Ochterski, R. L. Martin, K. Morokuma, O. Farkas, J. B. Foresman, and D. J. Fox, "Gaussian~16 Revision A.03," (2016), gaussian Inc. Wallingford CT.

[24] F. Santoro, A. Lami, R. Improta, J. Bloino, and V. Barone, "Effective method for the computation of optical spectra of large molecules at finite temperature including the Duschinsky and Herzberg–Teller effect: The Qx band of porphyrin as a case study," J. Chem. Phys. **128**, 224311 (2008), publisher: American Institute of Physics.

[25]J. N. Harvey, M. Aschi, H. Schwarz, and W. Koch, "The singlet and triplet states of phenyl cation. A hybrid approach for locating minimum energy crossing points between non-interacting potential energy surfaces," Theor Chem Acc **99**, 95–99 (1998).

[26]B. Gonon, A. Perveaux, F. Gatti, D. Lauvergnat, and B. Lasorne, "On the applicability of a wavefunction-free, energy-based procedure for generating first-order non-adiabatic couplings around conical intersections," J. Chem. Phys. **147**, 114114 (2017), publisher: American Institute of Physics.

[27]T. Etienne, X. Assfeld, and A. Monari, "Toward a Quantitative Assessment of Electronic Transitions' Charge-Transfer Character," Journal of Chemical Theory and Computation **10**, 3896–3905 (2014).

[28]T. Etienne, "Probing the Locality of Excited States with Linear Algebra," Journal of Chemical Theory and Computation **11**, 1692–1699 (2015).

[29]T. Etienne, "Towards rigorous foundations for the natural-orbital representation of molecular electronic transitions," arXiv preprint arXiv:2104.11947 (2021).

[30]T. Etienne, "Molecular electronic-structure reorganization: Analysis (mesra)," (2019, https://mesrasoftware.wordpress.com, accessed June 26, 2020).

[31]T. Le Bahers, C. Adamo, and I. Ciofini, "A Qualitative Index of Spatial Extent in Charge-Transfer Excitations," Journal of Chemical Theory and Computation **7**, 2498–2506 (2011).

[32]M. Head-Gordon, A. M. Grana, D. Maurice, and C. A. White, "Analysis of Electronic Transitions as the Difference of Electron Attachment and Detachment Densities," The Journal of Physical Chemistry **99**, 14261–14270 (1995).

[33]M. Gutmann, M. Gudipati, P. F. Schoenzart, and G. Hohlneicher, "Electronic spectra of matrix-isolated tolan: site selective one- and two-photon spectra," J. Phys. Chem. **96**, 2433–2442 (1992), publisher: American Chemical Society.

[34]Y. Amatatsu and M. Hosokawa, "Theoretical Study on the Photochemical Behavior of Diphenylacetylene in the Low-Lying Excited States," J. Phys. Chem. A **108**, 10238–10244 (2004), publisher: American Chemical Society.

[35]T. Suzuki, M. Nakamura, T. Isozaki, and T. Ikoma, ""Dark" Excited States of Diphenylacetylene Studied by Nonresonant Two-Photon Excitation Optical-Probing Photoacoustic Spectroscopy," Int J Thermophys **33**, 2046–2054 (2012).

[36]C. Ferrante, U. Kensy, and B. Dick, "Does diphenylacetylene (tolan) fluoresce from its second excited singlet state? Semiempirical MO calculations and fluorescence quantum yield measurements," J. Phys. Chem. **97**, 13457–13463 (1993), publisher: American Chemical Society.

[37]M. Hodecker, A. M. Driscoll, U. H. F. Bunz, and A. Dreuw, "Twisting and bending photo-excited phenylethynylbenzenes – a theoretical analysis," Phys. Chem. Chem. Phys. **22**, 9974–9981 (2020), publisher: The Royal Society of Chemistry.

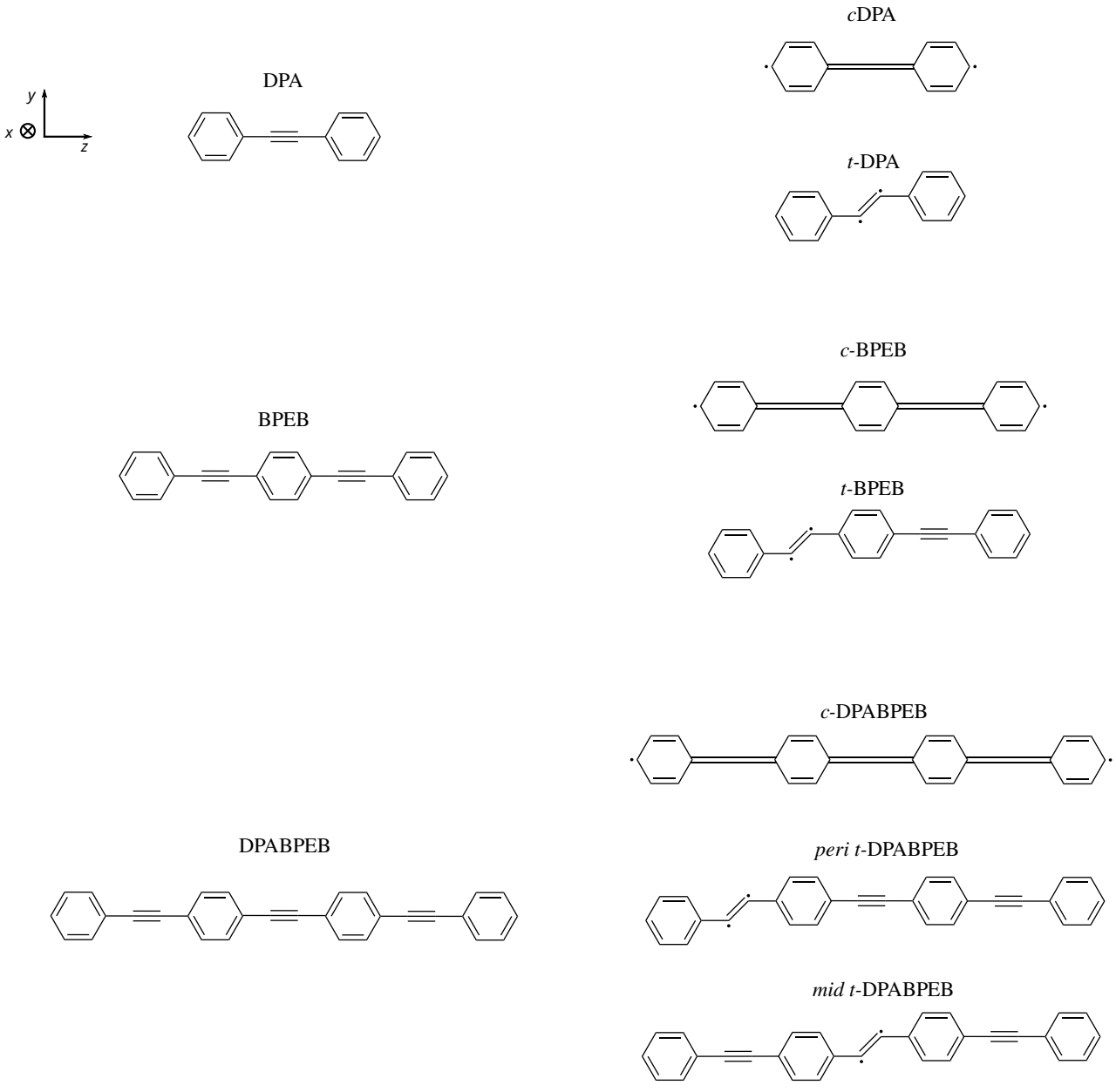

Figure 1. Lewis structures of DPA, BPEB, and DPABPEB in the ground electronic state (left column) and of their various isomers in the first adiabatic excited electronic states (right column).

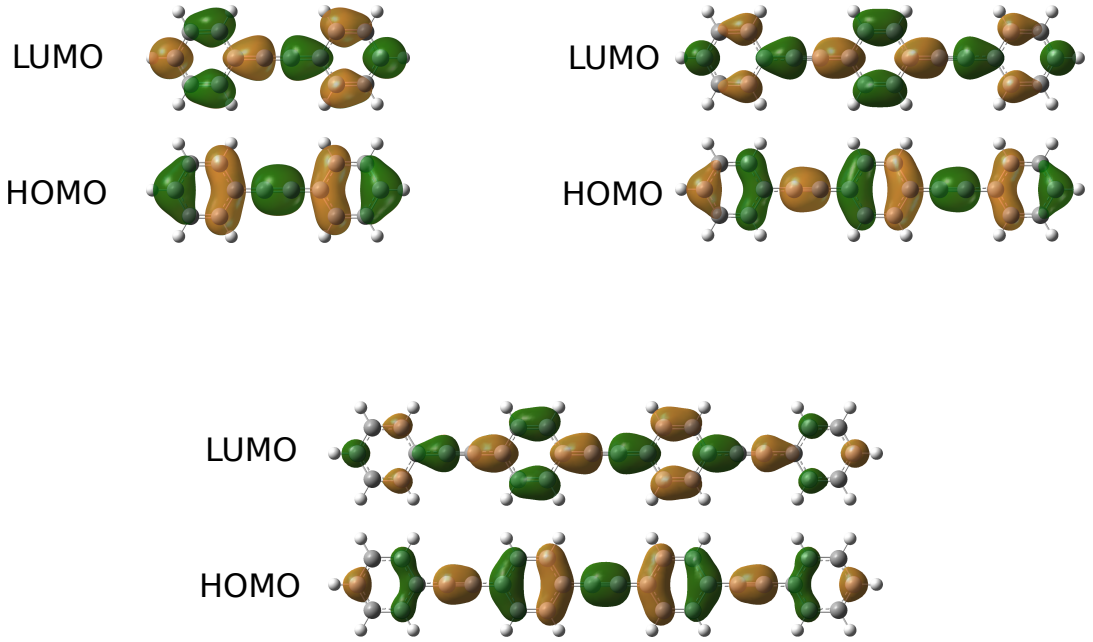

Figure 2. HOMOs and LUMOs at the cumulenic isomers of DPA, BPEB, and DPABPEB.

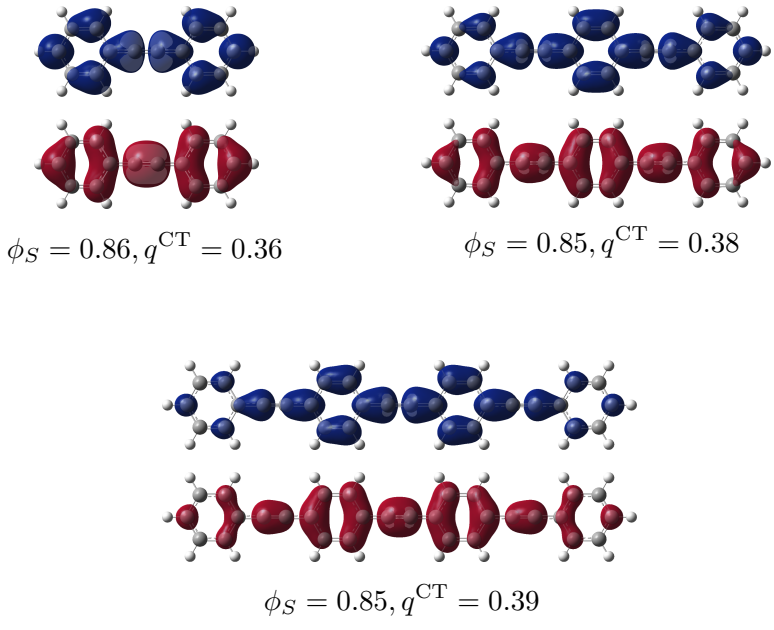

Figure 3. Attachment (in blue) and detachment (in red) densities obtained for the cumulenic isomers of DPA, BPEB, and DPABPEB, with corresponding values of the attachment-detachment-overlap density-based descriptor, ϕ_{S}, and charge-shift density-based descriptor, q^{CT}.

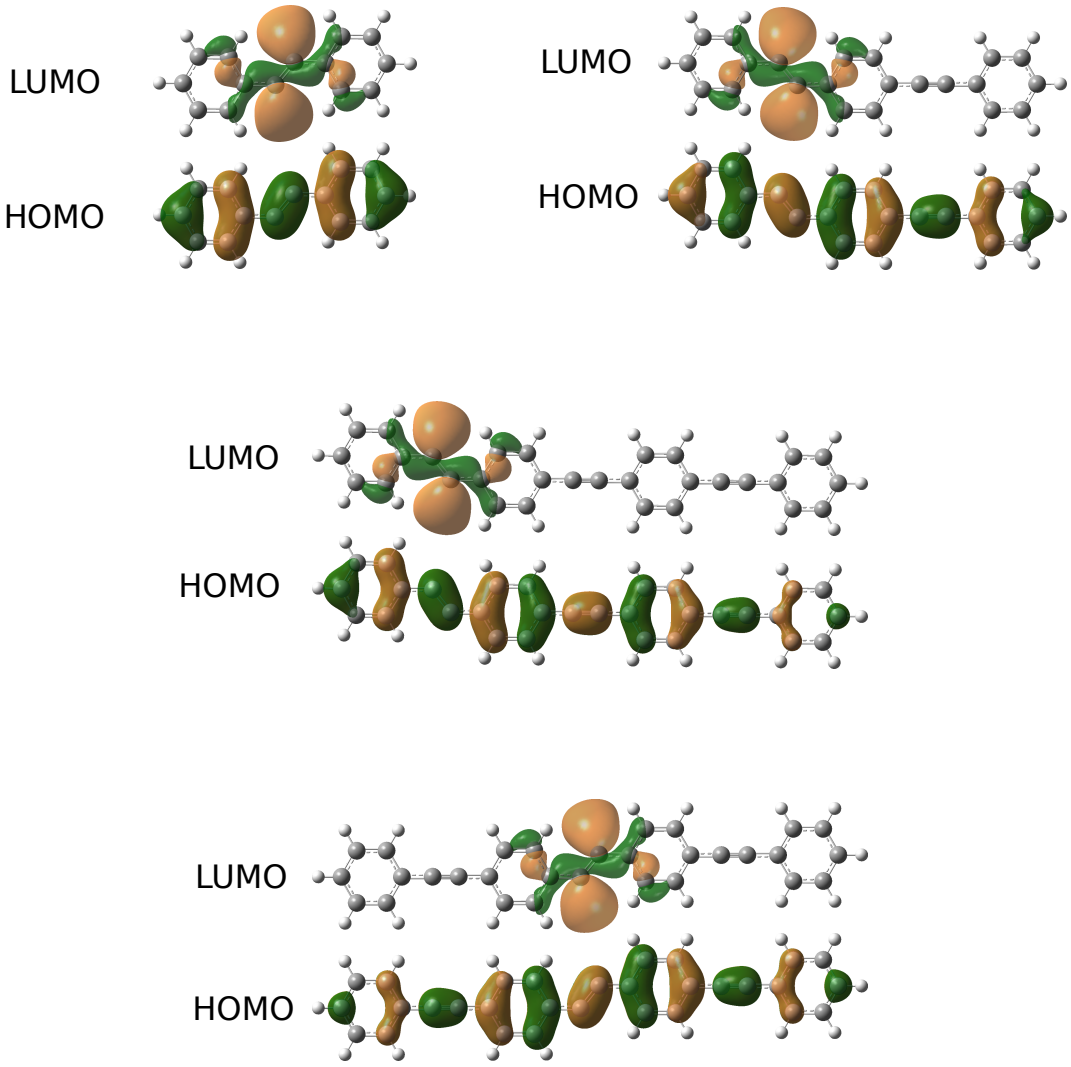

Figure 4. HOMOs and LUMOs at the *trans* isomers of DPA, BPEB, and DPABPEB.

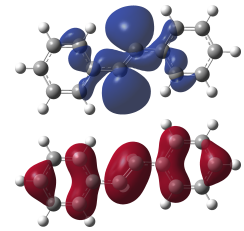

$\phi_S = 0.54, q^{\mathrm{CT}} = 0.74$

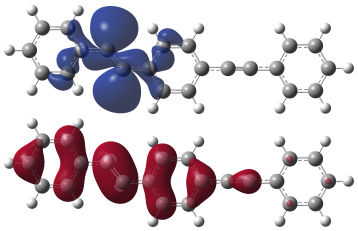

$\phi_S = 0.53, q^{\mathrm{CT}} = 0.74$

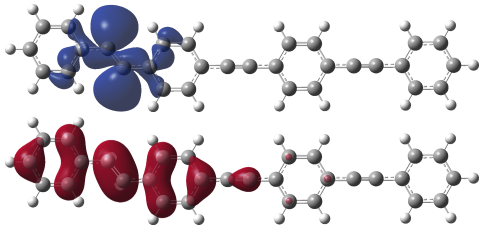

$\phi_S = 0.53, q^{\mathrm{CT}} = 0.74$

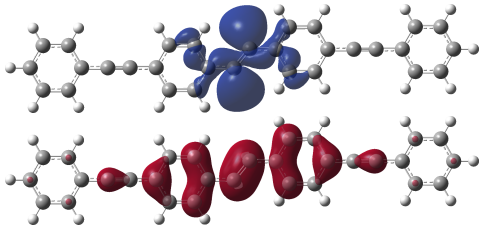

$\phi_S = 0.53, q^{\mathrm{CT}} = 0.75$

Figure 5. Attachment (in blue) and detachment (in red) densities obtained for the *trans* isomers of DPA, BPEB, and DPABPEB, with corresponding values of the attachment-detachment-overlap density-based descriptor, ϕ_{S}, and charge-shift density-based descriptor, q^{CT}.

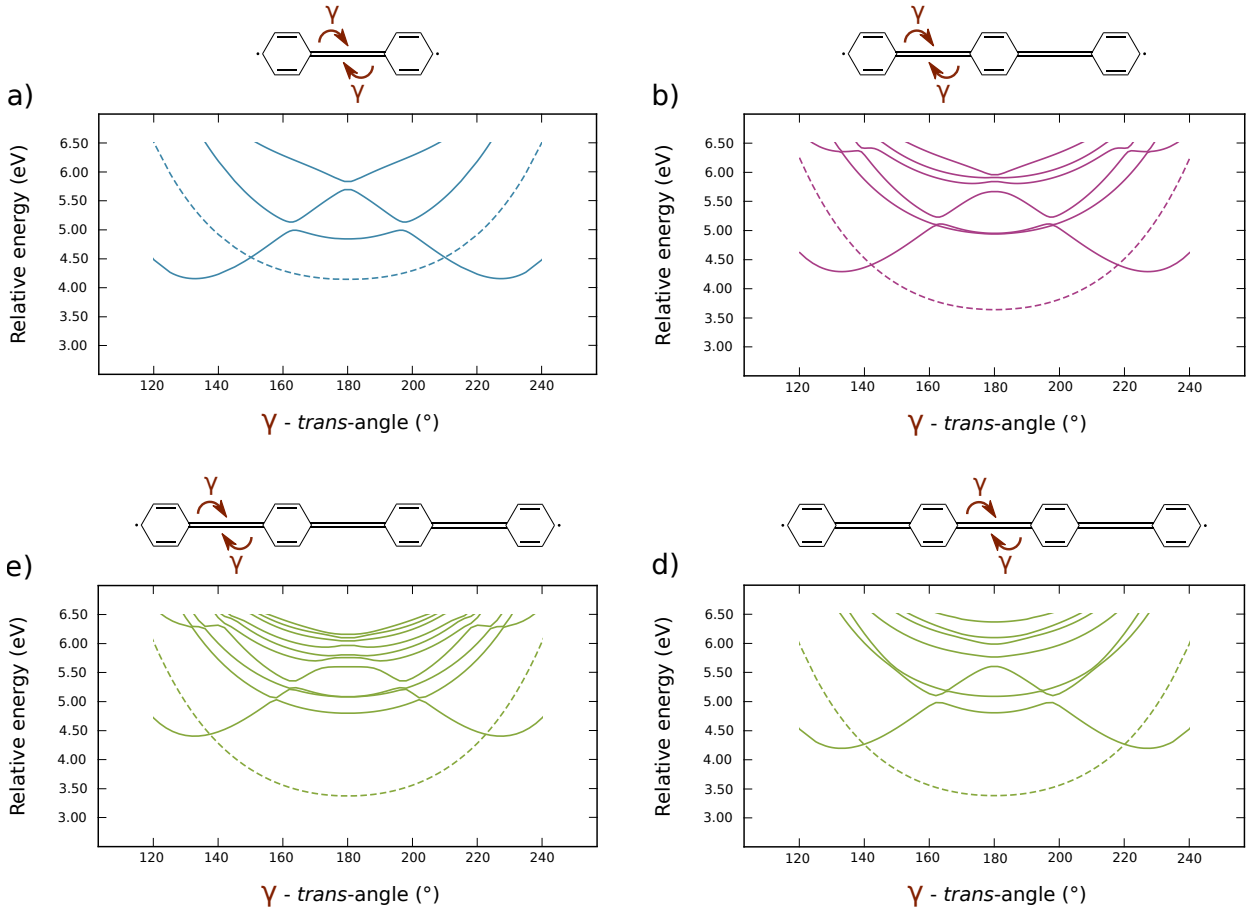

Figure 6. Rigid scans along the γ *trans*-bending angle from the equilibrium geometry of the bright cumulenic isomers in S_1. Dashed lines: bright states; plain lines: dark states. Blue corresponds to DPA, purple to BPEB, and green to DPABPEB.

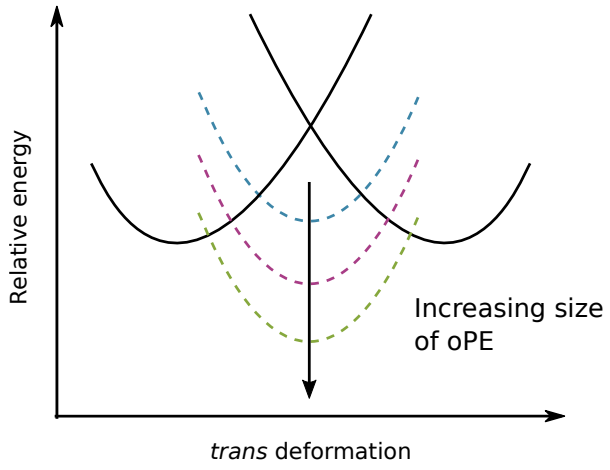

Figure 7. Schematic representation of the influence of the size of an oPE on the relative positions of bright and dark states and their crossings.

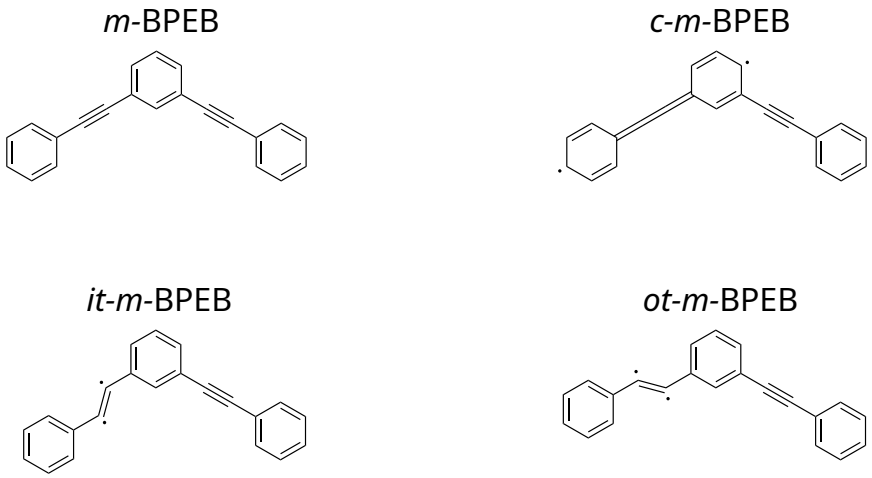

Figure 8. Lewis structures at the S_0 equilibrium geometry (*m*-BPEB) and in S_1 (*c*-*m*-BPEB, *it*-*m*-BPEB, and *ot*-*m*-BPEB).

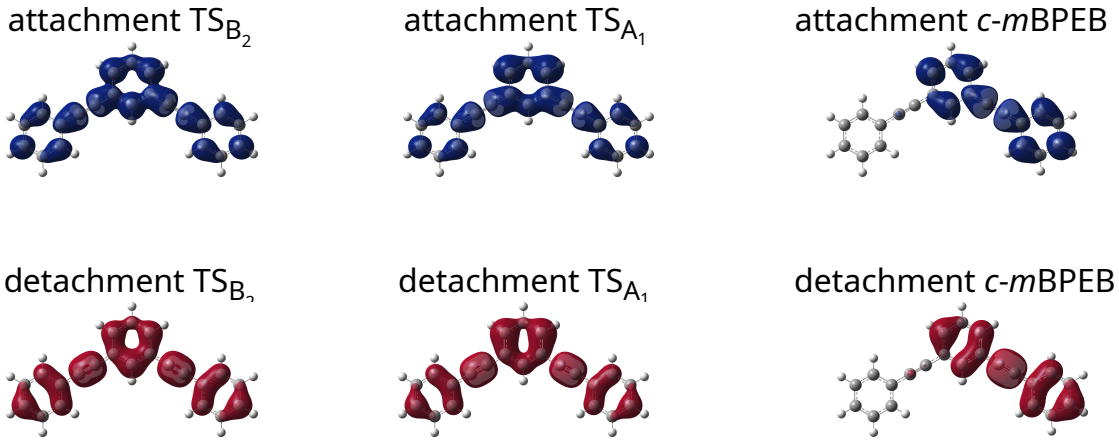

Figure 9. Attachment and detachment densities at both transition states, TS_{B_2} and TS_{A_1}, and at the S_1 minimum *c*-*m*BPEB.

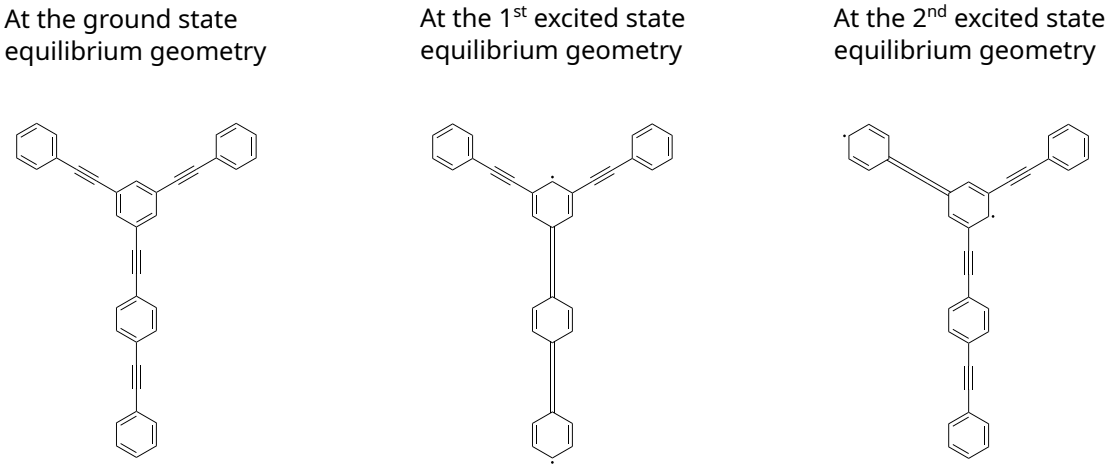

Figure 10. Lewis structures of *mb*-DPABPEB at the equilibrium geometries of the ground state, and first and second bright electronic states.

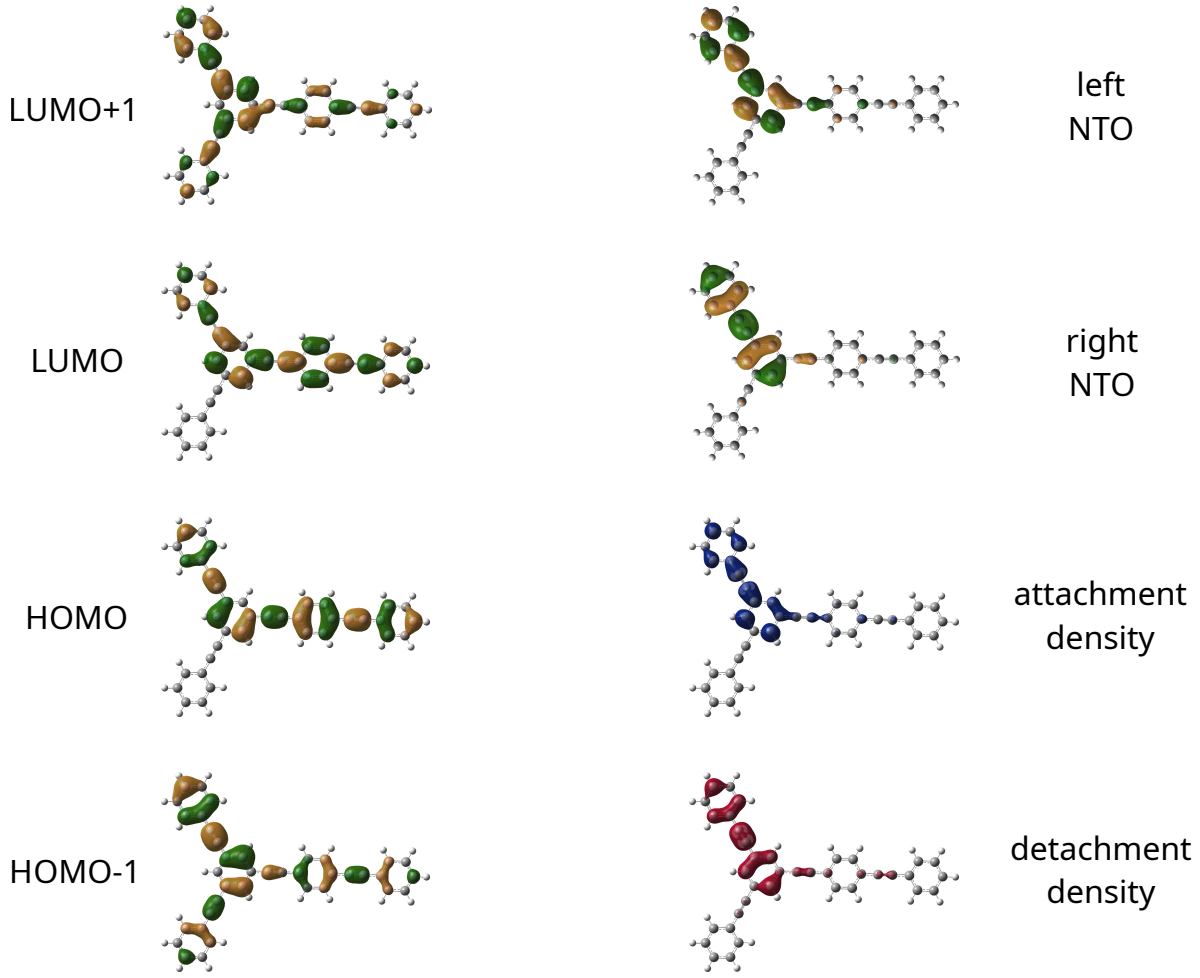

Figure 11. The four frontier orbitals (HOMO−1, HOMO, LUMO, and LUMO+1), the dominant pair of NTOs, and the attachment and detachment densities of *mb*-DPABPEB computed at the equilibrium geometry of the bright S_2 state of *mb*-DPABPEB.

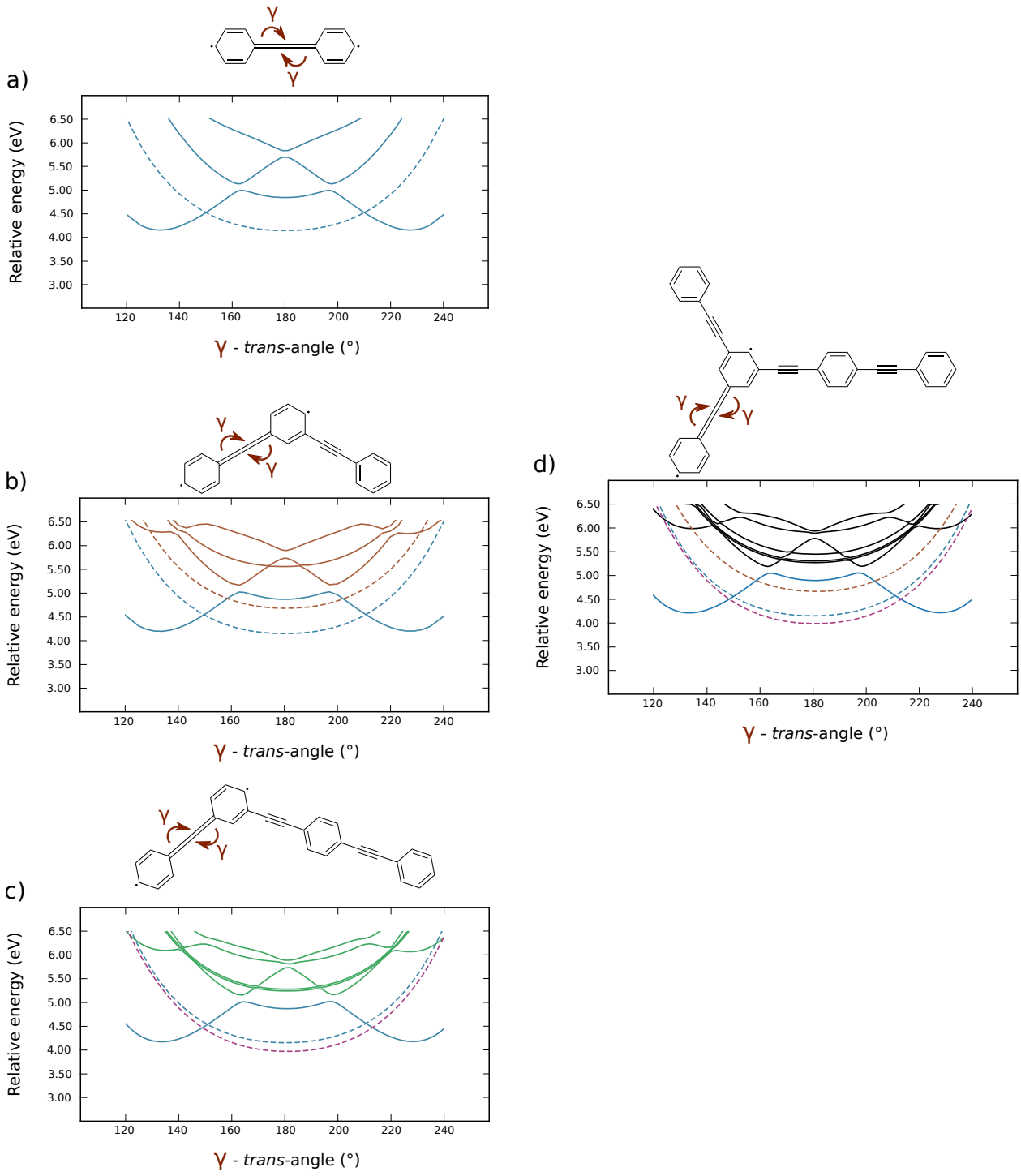

Figure 12. Rigid scans of DPA (a), *m*-BPEB (b), *m*-DPABPEB (c), and *mb*-DPABPEB (d) from the equilibrium geometry of the short-branch bright state (excitation-energy donor). Dotted lines correspond to bright states and plain lines to dark states. The blue/brown or purple colour code is used to draw attention on the main states of interest: excitations mostly localised on the cumulenic/alternated short branch or on the long branch, respectively (other colours are here for contrast only).

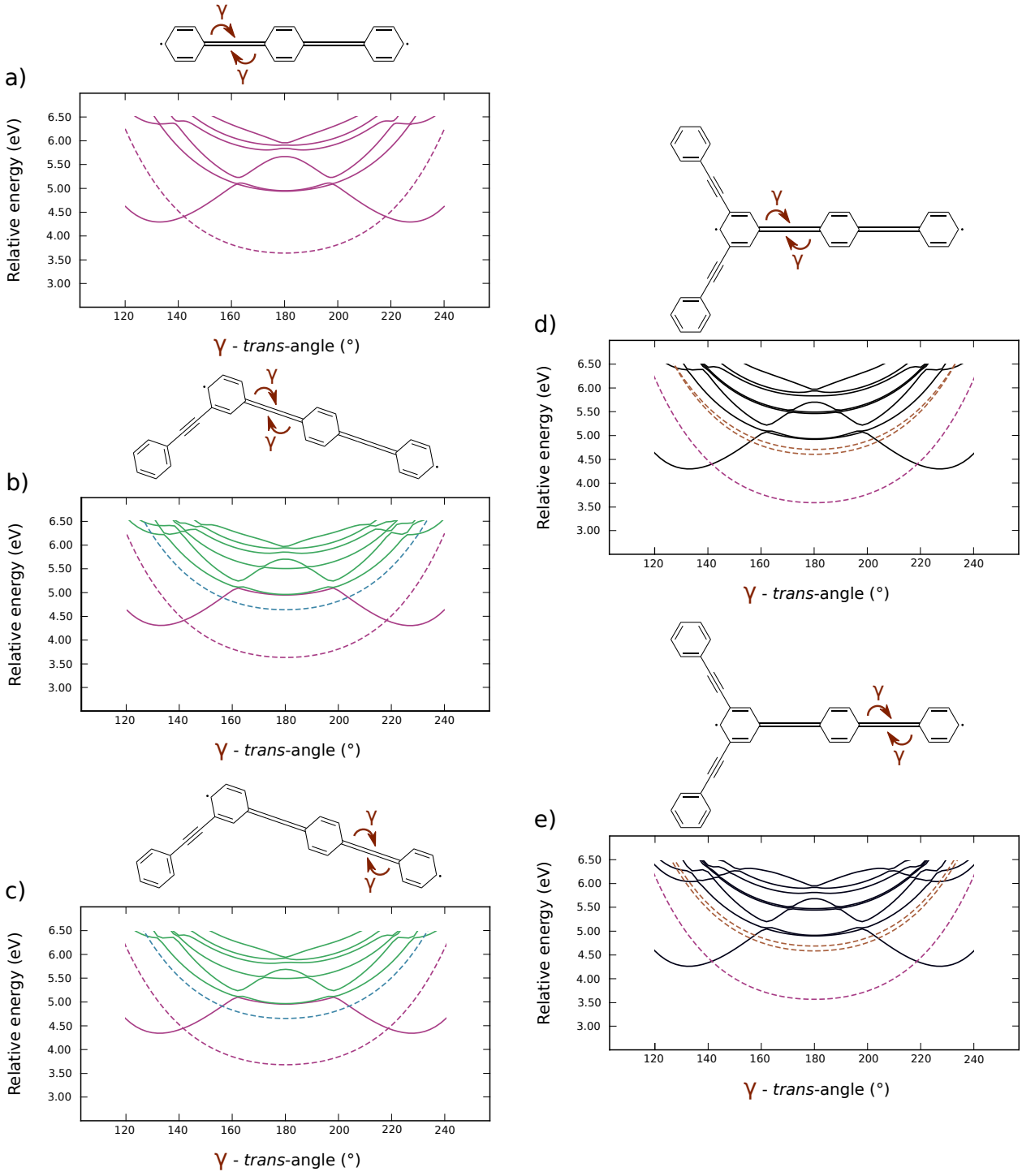

Figure 13. Rigid scans of BPEB (a), *m*-DPABPEB inside (b) and outside (c), *mb*-DPABPEB inside (d) and outside (e) from the equilibrium geometry of the long-branch bright state (excitation-energy acceptor). Dotted lines correspond to bright states and plain lines to dark states. The blue/brown or purple colour code is used to draw attention on the main states of interest: excitations mostly localised on the cumulenic/alternated short branch or on the long branch, respectively (other colours are here for contrast only).

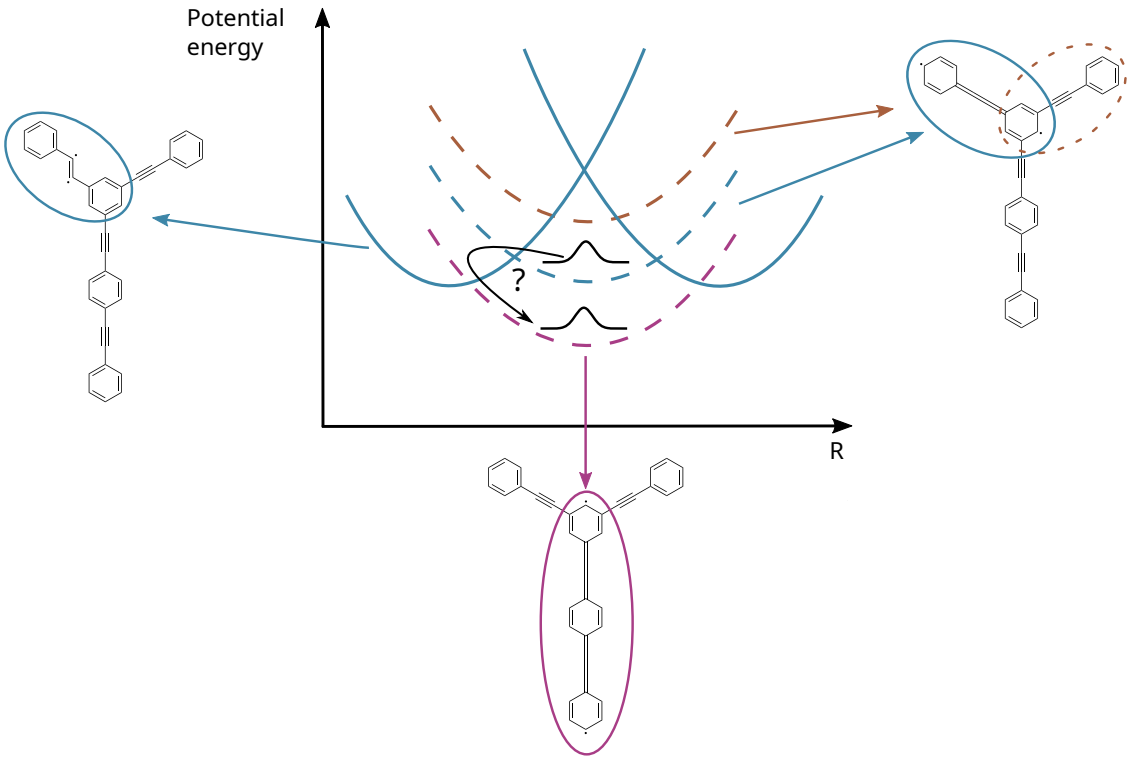

Figure 14. Schematic alternative pathway for EET in the first forked (phenylene ethynylene) dendrimer prototype along *R*, a composite de-activation coordinate.